Opal-based photonic crystal with double photonic bandgap structure

2000 J. Phys.: Condens. Matter 12 8221

(http://iopscience.iop.org/0953-8984/12/37/318)

J. Phys.: Condens. Matter **12** (2000) 8221–8229. Printed in the UK PII: S0953-8984(00)10736-2

Opal-based photonic crystal with double photonic bandgap structure

S G Romanov†, H M Yates‡, M E Pemble‡ and R M De La Rue§

† Ioffe Physical Technical Institute, 194021, St. Petersburg, Russia and Institute of Materials Science and Department of Electrical and Information Engineering, University of Wuppertal, 42097, Wuppertal, Germany
‡ Department of Chemistry, University of Salford, Salford M5 4WT, UK
§ Optoelectronics Research Group, Department of Electronics and Electrical Engineering, University of Glasgow, Glasgow G12 8QQ, UK

E-mail: romanov@uni-wuppertal.de

Received 5 January 2000, in final form 12 July 2000

Abstract. The interior surfaces of one part of a piece of artificial opal have been coated with GaP so that the remaining part of the opal crystal remains empty, thus forming a photonic heterostructure. Two Bragg resonances have been observed in the optical transmission and reflectance spectra. These two resonances were found to behave differently with changes in the polarization of the incident light and the angle of propagation of the light with respect to the (111) planes of opal. Depolarization of the light was observed to occur most effectively at frequencies within the stop-bands, apparently due to the re-coupling of the propagating electromagnetic wave to a different system of eigenmodes when it crosses the interface separating two parts of the double photonic crystal.

A new dimension has been given to the field of optoelectronic devices since the invention of photonic crystals in late the 1980s [1]. For the full potential of light channelling and 'moulding' to be achieved, the incorporation of several different photonic bandstructures in one photonic crystal is desirable. The basic construction block for this type of device is a photonic crystal with a double-photonic-bandgap (PBG) structure, for which the energy band diagram looks rather similar to that of an electronic heterojunction formed between two different semiconductors. Clearly the behaviour of a PBG heterostructure would be expected to differ dramatically from that of its electronic counterpart because the photons may occupy all the allowed states, both above and below the bandgap. Such multiple PBG structures could possibly be used, e.g. to isolate photonically the active zone of a PBG light source from areas with electrical contacts, to guide and to separate photons with different frequencies. Fabrication of such structures in one or two dimensions has become, in principle, a matter of routine [2], but it still appears to be a challenging task for three-dimensional photonic crystals.

We have explored the formation of double-PBG three-dimensional photonic crystals using the template approach [3]. In this case, the basis of the PBG structure is provided by synthetic opal, which consists of regularly packed silica balls. In bare opal the refractive index contrast (RIC) is as low as 1.45 to 1 and its PBG behaviour is far from complete. On top of this basic photonic crystal, a modified PBG structure can be formed in part of the opal by embedding a high refractive index (RI) semiconductor in the voids of the opal. Recently it has been

0953-8984/00/378221+09$30.00

shown that the PBG of opal can be enhanced significantly by the deposition of a thin layer of semiconductor on the inner surfaces of the opal [4–6]. The advantages of this treatment are the uniformity of the infill distribution and the preservation of free spaces in the opal for further treatment. In accord with theoretical simulations such coated opals could approach the omnidirectional PBG after removal of the silica skeleton of the opal [7, 8]. In this paper we discuss, qualitatively, the transmission and reflectance spectra of the prototype of a PBG heterostructure made from opal, one part of which is unfilled and the other part of which is loaded with GaP. In spite of the substantial anisotropy of the PBG behaviour in both sections of this composite photonic crystal, the case that we have studied is of definite interest, because some features of its behaviour will clearly be retained in the more advanced (complete PBG) structures which will be made in the future.

Opal is a three-dimensional diffraction grating consisting of closely packed silica balls which are arranged in a face-centred cubic (fcc) lattice. Synthetic opal with $D \approx 240$ nm and porosity $f_{Air} = 0.13$ was used. The impregnation of the free opal volume with 'guest' material is possible due to the interconnections between interstitial voids in opal [9]. The GaP growth process applied was atmospheric pressure MOCVD, using phosphine (Linde) and trimethyl gallium (Epichem) as precursors, in a similar manner to that used in our previous work with InP [10]. As opposed to the standard MOCVD method, the modified deposition uses lower growth temperatures (maximum 350 °C) and alternative addition of the precursors. In order to increase the GaP content in the opal the growth cycle was repeated three and five times respectively in different samples. Apparently, in the samples possessing low volume fraction of GaP the semiconductor clusters nucleate on adsorption centres (oxygen vacancies) on the surface of the silica balls of opal and the coating is composed of semiconductor nanoparticles [5]. In what follows we denote opal without semiconductor as air-opal and opal with GaP coating as GaP-opal.

The efficiency of the gas transported reaction process across an opal depends on a number of factors, including the temperature gradient and the diffusion rates for the precursors through the sample. In the case of an ideal fcc package of hard balls the free interstitial volume is 26% and the inter-void windows are wide enough to not affect the gas phase reaction. The reduction of the inner free volume down to 13% was achieved by depositing an amorphous silica from a silica–organic solution prior to infilling with the semiconductor. This pre-treatment increases the inner surface of the opal by factor of ten, which favours the absorption of metal–organic precursor. In such samples in-depth limitation of the GaP synthesis is observed. The exact reason for this effect is not known, but it may depend on the gas pressure, temperature and the cross-section of void interconnections. For example, in a one millimetre thick opal slab an approximately 300 micrometre thick core remains unprocessed while surrounded by a 200–300 μm thick 'skin' of GaP-infilled opal. Remarkably, the interface between the GaP-coated and unprocessed parts of the opal slab, where the concentration gradient is formed, is only a few micrometres thick zone as seen with an optical microscope. Pre-filling the voids with the amorphous silica makes a detailed investigation of the interface using electronic microscopy difficult because of the very rough surface of interstitial voids.

Samples for optical investigation have been prepared from the 'skinlike' infilled opal by polishing one side to form a sandwich structure: one face of the platelet was that of the GaP-loaded part, whereas the opposite face was the GaP-free part. Samples were in the shape of platelets between 0.15 and 0.3 mm thick, with the (111) planes of the opal package oriented along the surface. The sample surface was left rough enough (up to ten layers of balls) to eliminate the mirror reflectance in a studied spectral interval. Thus the system under study is a photonic crystal with a step in the effective refractive index at a plane crossing the sample volume. All three interfaces (two external and one internal) were parallel each other. The opals used

are polycrystals consisting of 50 to 100 μm large crystallites, where the common (111) growth plane is rotated by approximately $\pm 10^{\circ}$ around the (111) axis from one crystallite to the other.

Transmission and reflectance measurements were used to characterize the PBG structure of the (GaP-opal)–(air-opal) heterostructure. The spectra were measured for different angles, θ_{inc}, of incidence of the incoming monochromatic light with respect to the sample surface normal (the (111) axis). Only that part of the transmitted/scattered light, which was within a 2 degree divergence angle was recorded by the detector, while performing angle-resolved measurements. For measurements of the reflectance at oblique incidence, specular conditions were used ($\theta_{inc} = \theta_{scat}$ with respect to the surface normal). Two linear polarizers, one before and the other after the sample, were used to separate the transmission/reflectance spectra into s- and p-polarizations, as well as to examine the depolarization of the scattered light (p- and s-polarization denote the situations where the electrical field vector of the light is respectively in the plane of incidence and perpendicular to this plane). An illumination spot of 1 mm diameter has been used; correspondingly, the measured signal was averaged over hundreds of crystallites.

Figure 1(a) shows the transmission and reflectance spectra for light incident along the (111) direction of the opal package. The two minima/maxima in these spectra at $\lambda_1 = 571$ nm ($E_1 = 2.18$ eV) and $\lambda_2 = 543$ nm ($E_2 = 2.28$ eV) correspond to the Bragg scattering resonances from the same three-dimensional diffraction grating but with distinct regions possessing different RICs. These Bragg resonances demonstrate the presence of two stop-bands in the (111) direction. The corresponding schematic for the photonic crystal is shown in figure 1(c). The transmission spectra were measured for light incident on opposite faces of the opal platelet. The transmission is insensitive to changes in the optical propagation direction: the resonance from the air-opal part at 2.28 eV always dominates over the resonance from the GaP-opal part of the crystal, at 2.18 eV. With increases in the thickness of the air-opal part of the sample, the 2.18 eV diffraction dip becomes much less pronounced because it represents a progressively smaller part of the total attenuation. The magnitude of the light reflected back from both surfaces of the sample at the Bragg resonance frequency is about the reflectance signal from the spectroscopic standard of the diffuse reflectance. The relative bandwidth of the Bragg resonance in the air-part of the sample is $\Delta E/E_0 \approx 0.053$, where ΔE is the full bandwidth at half height and E_0 is the central frequency of the peak, which value is close to that obtained from a band stricture calculations for bare opal [12]. In the GaP-filled part the bandwidth is slightly higher, $\Delta E/E_0 \approx 0.068$. Further increase of the bandwidth is expected for larger filling fraction of GaP.

The transmission spectrum figure 1(b) is superimposed on a rapidly decreasing background. It is common experience [11], that on the 'red' side of the stop-band this background is due to Rayleigh scattering, for which the standard wavelength-dependent transmission, $T \propto \lambda^4$, is plotted as the dashed line. On the 'blue' side of the stop-band, a much more rapidly declining background, with its exponent estimated as being in the range eight to ten, was observed and assigned, tentatively, to absorption by the GaP infill, which becomes large at approximately 2.4 eV.

The obvious reason for the two resonances to appear at different wavelengths is the difference in the RI of the loaded and the empty parts of the opal heterostructure. The Bragg condition $\lambda_{Bragg} = 2n_{eff}d$, where $d = 0.816D$ is the interplane distance in the (111) direction, allows extraction of an effective RI value of $n_{eff3} = 1.47$ for the GaP-filled part of the structure and $n_{eff2} = 1.41$ for the unfilled part. Numerical simulations of the PBG structure of opals indicate that the Bragg resonance estimates correctly the central frequency of the lowest stop-band, at least for the wave-vectors between L and U points of the Brillouin zone in the case of crystals with moderate RI contrast (see, for example, [12, 13]). On the other hand, the

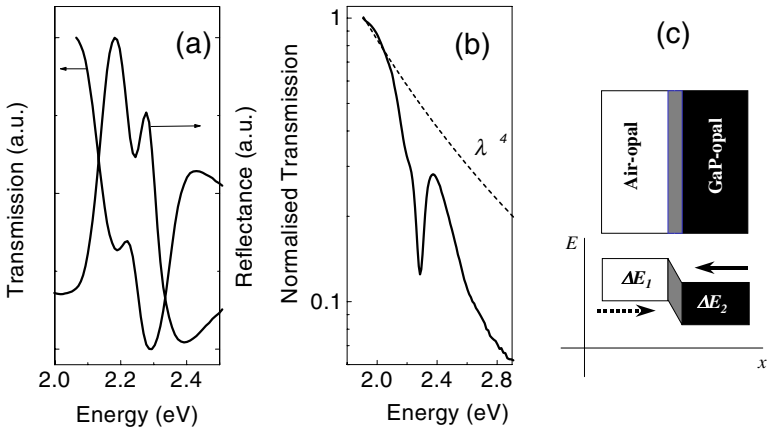

Figure 1. (a) Transmission and reflectance of the opal double photonic crystal. The Rayleigh background has been subtracted from the transmission curve. (b) Measured transmission spectrum and λ^4 curve. (c) Schematics of the double photonic crystal and its photonic energy band diagram.

RI of the composite can be estimated in the long-wavelength limit using simplified effective medium approach as $n_{eff} = \sum_i n_i f_i$, where i is the index of a component. Simultaneous use of both models has been justified in the case of low-RI-contrast opal-based photonic crystals†. Correspondingly, the volume fraction of the deposited GaP can be estimated as $f_{GaP} \approx 3\%$ for $n_{GaP} = 3.42$ in this wavelength range [6]. The air-part of the sample apparently exhibits an effective RI somewhat higher than that of bare opal ($n_{eff1} = 1.39$), which suggests the existence of some deposited material in this part of the platelet. However, we assume that negligible GaP formation has occurred because this part of the sample retains its white colour.

An important assumption can be drawn about the role of the transition region between the GaP- and air-parts of the opal. If a thick transition region were formed, both resonances would certainly have highly broadened transmission spectra because this region can be considered as a high-defect-density zone [15]. This assumption supports the estimate of the interface width made with an optical microscope.

Figure 2 illustrates the trend in evolution of the Bragg resonances with increased GaP loading. In the case of the heavier loaded opal these two resonances appear more clearly separated because of the larger shift of the GaP-opal Bragg peak. The sample with higher GaP occupancy shows a much deeper minimum in transmission for similar layouts of the GaP- and air-parts (figure 2). This observation is in agreement with numerical simulation of the optical transmission along the (111) direction in coated opals, which indicates that, after the initial stages of coating, the optical attenuation increases in the coated opal [12]. Scatterers in GaP-opal are semiconductor quasi-spheres with air core. In the sample possessing 3 vol% of GaP the infill occupies about 22% of the interstitial void volume. This coating is thick enough to raise the effective RI of the GaP shell to approximately 1.59, which value exceeds the RI of silica, 1.45, where these scatterers are immersed. In GaP-opal with about 5 vol% of GaP the infill occupies 39% of its void volume and the effective RI of scatterers is 1.99. In other words the coated opal scatters the electromagnetic waves as effectively as the inverted opal [6].

† The accuracy of the effective medium approach within a few per cent has been proved by numerous experiments and simulations. See, for example, [14]. Moreover, at angles of incidence higher than 40–50° the deviation from the Bragg law reflects the branching of the dispersion bands, e.g. at the crossing point of bands related to (111) and (200) planes.

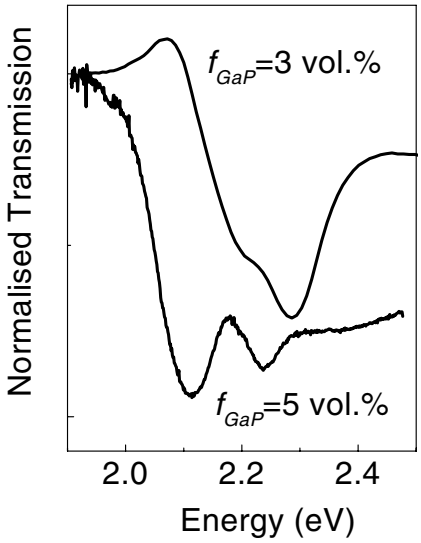

Figure 2. Normalized transmission spectra of samples with five ($f_{GaP} \approx 5$ vol%) and three ($f_{GaP} \approx 3$ vol%) GaP deposition cycles. The Rayleigh background has been subtracted.

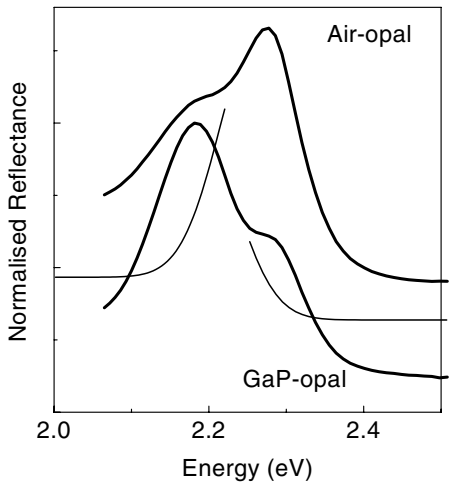

Figure 3. Reflectance spectra from opposite faces of the photonic crystal. Thin lines indicate the Gaussian lineshape of the dominant resonance in each case.

The reflectance spectra taken from the opposite faces of the photonic heterostructure are dominated by the Bragg resonance from that part on which the light is incident (figure 3). This behaviour occurs because the incident light is mostly scattered by the near-surface region of the photonic crystal. Both peaks appear superimposed in the reflectance spectrum because in the frequency range where the shadowed part of the heterostructure scatters the light resonantly the illuminated part scatters the incident light diffusely. Correspondingly, the Bragg peak from the shadowed part of the double crystal is partially attenuated by scattering in the illuminated part. The Gaussian lineshape of the main resonance has been separated from the

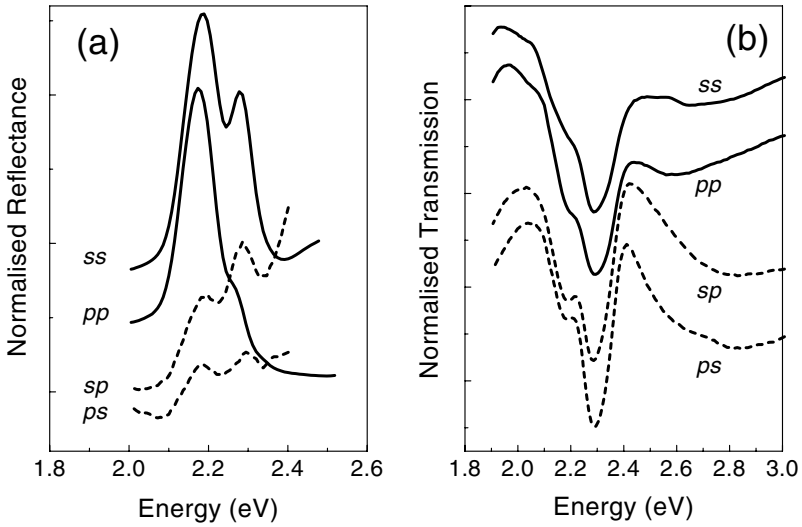

Figure 4. Reflectance (a) and transmission (b) spectra for different polarizations of the incident and scattered light at $\theta = 0^\circ$. The polarization of the incident/scattered light is indicated on the curves: the first letter shows the polarization of the incident light and the second one the polarization of the detected light.

spectra in figure 3 to show that these two stop-bands overlap considerably when measurements are made along the (111) direction. Correspondingly, this broadens the combined bandgap and achieving a heavier loading of the opal with the high-index GaP the combined transmission characteristic can look more complex.

The centre frequencies and the relative resolution of the stop-bands depend on the polarization of the incident and scattered light. In what follows we shall use a two-letter notation for the light polarization—the first letter refers to the incident light and the second refers to the scattered/transmitted light. The relative intensities of resonances at 2.18 eV and at 2.28 eV appear different for the pp-polarized and ss-polarized light (figure 4(a)). In a complementary fashion, the 2.18 eV dip in the transmission spectrum for pp-polarized light is stronger than for ss-polarized light (figure 4(b)). Correspondingly, we may assume that the diffraction for the p-polarized light occurs more effectively in GaP-opal, whereas the air-opal diffracts more effectively the s-polarized light. To what extent this difference relates to the different eigenmode structure of these parts of photonic crystal is a matter for further simulations.

Some depolarization was noticed in the light scattered by the heterostructure. In order to evaluate this process, the transmission and reflectance spectra were detected for cross-aligned entry and exit polarizers. The intensity of the depolarized component appears to be reasonably small—the ratio of the transmission intensities at 2 eV (frequency below the stop-band edge), $I_{sp}/I_{ss} \approx 1/1500$ and $I_{ps}/I_{pp} \approx 1/5000$, produces an estimate of the depolarization level. The spectra in figures 4(a) and (b) show similar Bragg peaks in parallel and cross-polarization. The depolarization rate was observed to be relatively weak in reflectance and, moreover, the Bragg resonances do not greatly exceed the background scattering level. In contrast, the Bragg resonances in the transmission spectra appear relatively better resolved in cross-polarized light than in parallel-polarized light. This observation suggests strongly that the depolarization occurs when the electromagnetic waves cross the interface.

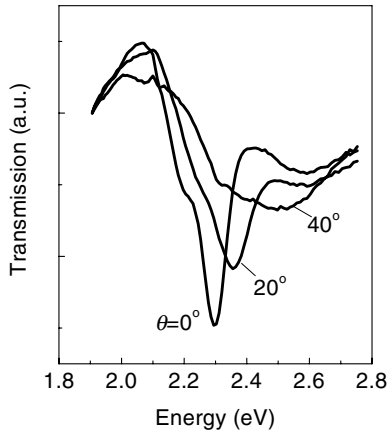

Figure 5. Transmission spectra at $\theta = 0$, 20 and 40° angles of incidence with respect to the (111) axis of the opal sample. The Rayleigh background has been subtracted.

Obviously, the mode structure of the electromagnetic field is different in bare and coated opals. This assertion holds because the layout of the unit cell in the coated opal differs from that of the direct opal [7] and the maxima of the electrical field in the lowest eigenmode of the photonic crystal occur at either the balls or the shells, whichever has the higher RI. Thus, at the interface between the two spatially distinct parts of the photonic crystal a field redistribution takes place, which process can be described in terms of coupling between two different mode structures. Correspondingly, the depolarization is the result of re-coupling of the propagating light from the eigenmodes of the air-opal to those of its replica and vice versa.

The minima in the transmission spectrum gradually collapse if the optical propagation direction deviates substantially from the (111) axis—and the two resonances merge into a single broad band (figure 5). The combined relative full stop-band linewidth taken at the half height $\Delta E/E_0$ is approximately 8% at $\theta = 0^\circ$ and approximately 15% at $\theta = 40^\circ$ (figure 5), thus exceeding the 5% bandwidth of the resonance in the reflectance spectrum for air-opal itself [16]. The increased separation of Bragg resonances in the photonic crystal heterostructure occurs because the two follow their own angular dispersion curves, which is stronger for air-opal as compared with GaP-opal.

The dominating diffraction resonance gradually overtakes the lesser diffraction resonance as the angle of incidence increases (figure 6). This happens because if the angle increases, the light path through the illuminated part of the heterostructure becomes higher and, in proportion, the attenuation of the diffraction resonance from the shadowed part increases.

In conclusion, we have investigated a photonic crystal containing two regions with different photonic band-structure by selective synthesis of GaP in one part of a synthetic opal sample. The appearance of the stop-band was studied via the light scattering from this sample in directions around the (111) axis of the opal lattice. In spite of both parts of the photonic crystal demonstrating incomplete photonic bandgap behaviour, we have been able to observe the general features which are inherent in all 'filled–empty' types of opal-based photonic crystal heterostructures: (a) the spectral separation and/or the overlap of the two bandgaps, as they appear along the same direction of observation, depends on the difference between the RI contrasts in the two parts of the crystal, (b) in the transmission spectrum the appearance of the two scattering resonances depends on the characteristic attenuation in each part of the heterostructure but it can be balanced by changing the relative thickness of these parts, (c) two

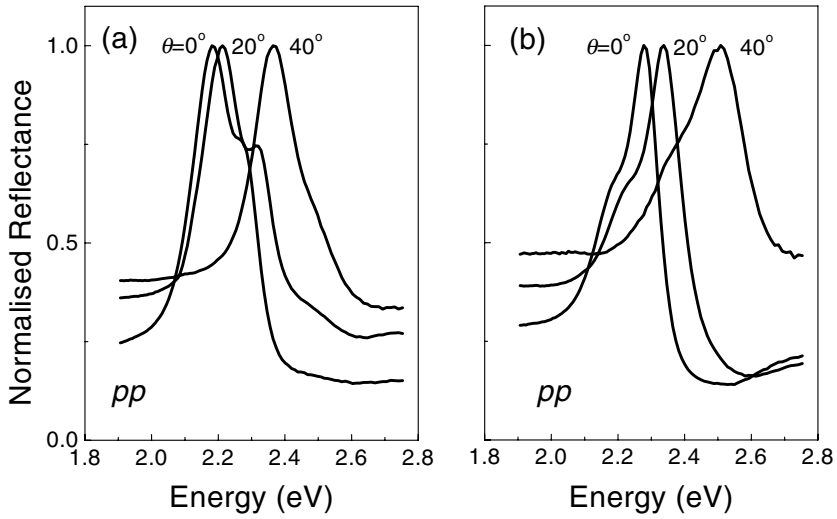

Figure 6. The normalized reflectance spectra for pp-polarization from (a) the GaP-opal face and (b) the air-opal face of the double photonic crystal at $\theta = 5$, 20 and 40°.

parts of the photonic heterostructure show the different anisotropy, (d) the direct and inverted opal structures respond differently to changes in the optical polarization, which property reflects the difference in scattering process within the unit cell, (e) depolarization of the electromagnetic waves takes place when they re-couple from the eigenmodes of the opal to that of the replica.

The structural quality of the studied photonic crystals is insufficient to observe fine features in diffraction properties, e.g. the band branching at the U point of the Brillouin zone [17] or mode coupling over the interface. However our experiment can be considered as a proof of principle. Advanced approach towards photonic crystal heterostructures can be explored using recently emerged thin opaline films [18]. This technology allows the successive 'epitaxial' deposition of layers of spheres; moreover, the opaline film can be modified, e.g. infilled and/or inverted, prior to the sedimentation of the next layers. In this case a well defined interface can be achieved with an abrupt change of the PBG structure.

Acknowledgments

This work was supported in part by the Leverhulme Trust (grant No F/179/AK), the Engineering and Physical Sciences Research Council (EPSRC grant No GR/M16542) and the Russian Foundation for Basic Research (grant 99-02-18156). The optical measurements were carried out at Glasgow University.

References

[1] Yablonovitch E 1987 *Phys. Rev. Lett.* **58** 2059
John S 1987 *Phys. Rev. Lett.* **58** 2486
[2] Krauss T and de la Rue R 1999 *Progr. Quantum Electron.* **23** 51
[3] Romanov S G and Sotomayor Torres C M 1999 *Handbook of Nanostructured Materials and Technology* vol 4, ed H S Nalwa (New York: Academic) ch 4, pp 231–323
[4] Romanov S G, Johnson N P, Yates H M, Pemble M E, Butko V Y and Sotomayor Torres C M 1997 *Appl.Phys.Lett.* **70** 2091

[5] Miguez H, Blanco A, Meseguer F, Lopez C, Yates H M, Pemble M E, Fornes V and Mifsud A 1999 *Phys. Rev.* B **59** 1563
[6] Romanov S G, Yates H M, Pemble M E and de la Rue R M 2000 *J. Phys.: Condens. Matter* **12** 339
[7] Busch K and John S 1998 *Phys. Rev.* E **58** 3896
[8] Moroz A and Sommers C 1999 *J. Phys.: Condens. Matter* **11** 997
[9] Balakirev V G, Bogomolov V N, Zhuravlev V V, Kumzerov Y A, Petranovsky V P, Romanov S G and Samoilovich L A 1993 *Crystallogr. Rep.* **38** 348
[10] Yates H M, Flavell W R, Pemble M E, Johnson N P, Romanov S G and Sotomayor Torres C M 1997 *J. Cryst. Growth* **170** 611
[11] Vlasov Yu A, Astratov V N, Karimov O Z, Kaplyanskii A A, Bogomolov V N and Prokofiev A V 1997 *Phys. Rev.* B **55** R13 357
[12] Reynolds A, López-Tejeira F, Cassagne D, García-Vidal F J, Jouanin C and Sánchez-Dehesa J 1999 *Phys. Rev.* B **60** 11 422
[13] Blanco A *et al* 2000 *Nature* **405** 437
[14] Vos W L, Sprik R, von Blaadren A, Imhof A, Lagendijk A and Wegdam G H 1996 *Phys. Rev.* B **53** 16 231
Yannopapas V, Stefanou N and Modinos A 1998 *J. Phys.: Condens. Matter* **9** 10 261
[15] Vlasov Yu A, Kaliteeveski M A and Nikolaev V V 1999 *Phys. Rev.* B **60** 1555
[16] Romanov S G, Fokin A V and de la Rue R M 1999 *J. Phys.: Condens. Matter* **11** 3593
[17] Romanov S G, Maka T, Sotomayor Torres C M, Muller M and Zentel R 2000 *Synth. Met.* at press
Romanov S G, Maka T, Sotomayor Torres C M, Muller M, Zentel R, Manzanares J, Cassagne D and Jouanin C, submitted
[18] Xia Y, Gates B, Yin Y and Lu Y 2000 *Adv. Mater.* **12** 693–6